Integrated Distributed Acoustic Sensing and Communication in Coherent Passive Optical Network Transceiver Using Digital Subcarrier Multiplexing

L. Ebner[1,2], J. L. Moreno Morrone[1], R. Emmerich[1], A. Moawad[1,2], J. K. Fischer[1], R. Freund[1,2]

[1] Fraunhofer Heinrich-Hertz-Institute, Einsteinufer 37, 10587 Berlin, Germany,
[2] Technical University of Berlin, Straße des 17. Juni 135, 10623 Berlin, Germany

Abstract— **We present a comprehensive experimental and numerical investigation of integrated sensing and communication systems for coherent passive optical networks, wherein distributed acoustic sensing probes are digitally multiplexed in downstream transmission. The transmission quality and the influence of laser linewidth within a single transceiver architecture are systematically examined. Additionally, the system's capability to detect external vibrations representing potential threats to the fiber infrastructure is evaluated, demonstrating its potential for early warning of fiber interruptions and enabling resilient network operations.**

Keywords—Fiber Sensing, Integrated Sensing and Communication, Passive Optical Network, Distributed Acoustic Sensing, Optical Access Networks, Resilient Networks, Real Time Monitoring.

I. Introduction

In the last two decades the growth of individual network traffic has led to a vast expansion of the fiber to the home network [1]. Recent trends show that this fiber infrastructure can concurrently operate as a sensor within its deployed area. Especially distributed acoustic sensing (DAS) has gained momentum, because of its ability to spatially resolve external forces [2]. Besides optical network monitoring, some applications in urban areas for DAS include both traffic and structural health monitoring and surveillance of water flow and seismic activities [3].

Since modern optical communications usually use a bandwidth in the range of GHz and DAS sensing probes are in the range of MHz, a combined usage of the deployed fiber without a major penalty in transmission quality is possible. Recent works have demonstrated wavelength division multiplexing (WDM) systems, where the communication channel and sensing channel are created in separate devices and coupled in the fiber [4]. In [5] an integrated communication and sensing (ISAC) scheme is presented which inserts linear frequency modulated (LFM) sensing pulses into the header of the communication signal using a shared transmitter. However, this transmitting scheme cannot be detected together with the upstream communication channels in passive optical networks (PON).

Currently the discussion about the standardization of the next generation PON is ongoing in the ITU study group 15, where integration of DAS sensing in very high speed PON (VHSP) transceivers is investigated [6,7]. To maximize the cost efficiency of the sensing integration, the DAS system is integrated in the optical line terminal (OLT). Therefore, the need for expensive low linewidth lasers is minimized, and the multiple optical network units (ONU) can use conventional communication lasers. Typically, PON systems use time division multiple access (TDMA) to facilitate the upstream traffic of multiple users. Future systems could adopt time frequency division multiple access (TFDMA) to enable the concurrent transmission of multiple digital subcarriers (DSC) within a shared optical spectrum, providing enhanced flexibility in resource allocation [8].

In this work we propose an ISAC system, which digitally multiplexes a DAS sensing probe into the spectral gap between two neighboring subcarriers of the downstream signal. This scheme allows for a joint reception of the backscattered DAS signal together with the upstream communication signal in the OLT, since the sensing probe is adjacent in frequency and overlapping in time to the communication subcarriers. Furthermore, the power relation between the sensing and communication subcarrier in the transmitter is evaluated in terms of transmission quality and probability of detection of vibration events analytically and experimentally. By means of this analysis we provide a tradeoff to determine the power distribution and the impact of laser linewidth in an ISAC transceiver.

II. Simulation Setup

In Fig. 1) the simulation setup of the introduced ISAC architecture is depicted. The OLT is modeled as follows. Four 8 GBd polarization division multiplexed (PDM) quadrature phase shift keying (QPSK) digital subcarriers are created and then digitally multiplexed together with a sensing probe, a coded 500 MBd PDM binary phase shift keying (BPSK) pulse, using Hilbert transformations. BPSK sensing pulses are used, because they have a homogeneous spread in the time-frequency plane [4]. The sensing to telecom power ratio (STPR) is defined in [5] as the power distribution between the communication signal and the sensing probe in a joint transmitter. In our setup, it is designed variably to investigate its impact on the transmission quality and detection probability of an external vibration event. The combined signal is then modulated onto the 1550 nm optical carrier. Please note that the output power is fixed at 0 dBm. The physical characteristics of the fiber model include group velocity dispersion (GVD), polarization mode dispersion (PMD) and fiber nonlinearities to calculate the effects on forward propagation of the communication signal.

Additionally, the fiber includes the effect of Rayleigh scattering through the introduction of minor changes in the refractive index along the propagation axis of the launched optical signal, which scatters back a small amount of the incident light. Since the scatterers' location shifts slightly

978-3-903176-78-2 © 2026 IFIP

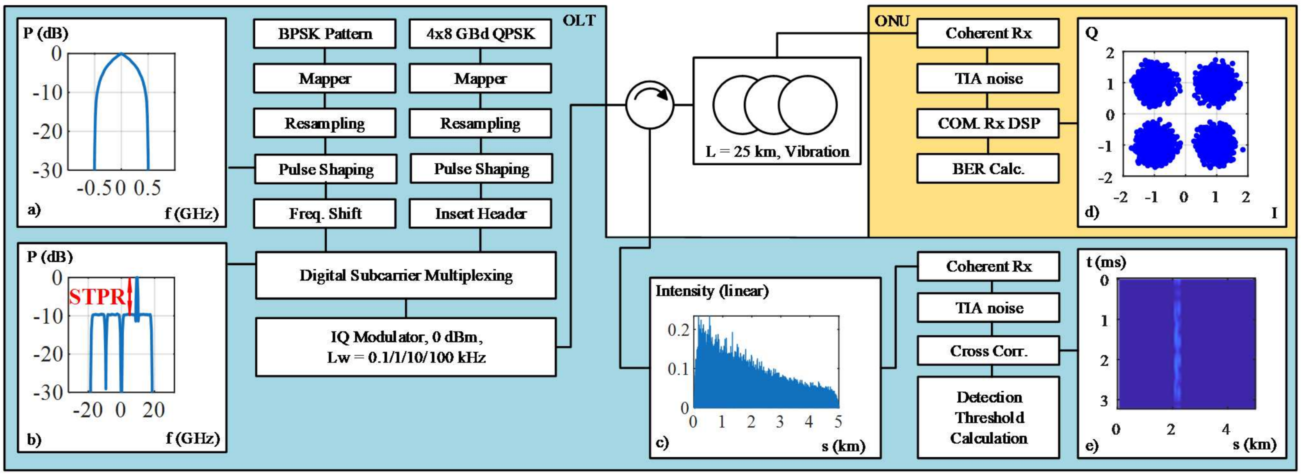

Fig. 1: Simulation Setup of ISAC using frequency shift and SCM in the transmitter and coherent reception (Rx) of the sensing probe in the OLT and coherent Rx in the ONU. For data transmission 4 digital subcarriers with 8 GBd PDM-QPSK are used. A 500 MBd PDM-BPSK pulse train is used as a sensing probe. The sensing in a) and combined spectra in b) with an STPR of -10 dB are shown. c) displays a backscattered trace of a 5 km fiber after reception. d) shows the constellation at the ONU (SNR = 10 dB) and e) the cross-correlation result of a vibration event at 2.8km.

dependent on external forces, a repeated probe can detect an underlying vibration frequency. The model is based on [9], where the impulse response of the Rayleigh backscattering channel is modeled as the sum of finite scatterers in the fiber. The location of vibration varies randomly with a uniform distribution to enable 500 Monte Carlo simulations of detection sensitivity. The backscattered signal is coherently detected in the OLT. Then the electrical amplifier noise, governed by the thermal noise in the transimpedance amplifier (TIA), is added. At high frequencies, it is considered as white noise [10]. The sensing signal is demultiplexed to recover the sensing probe. After cross correlation with the sent sensing sequence the location of the perturbation is extracted calculating the derivative over multiple probe signals and extracting its peak.

In the ONU, after coherent detection and TIA noise the GVD is compensated for and then the signal is demultiplexed. The recovered subcarriers are independently fed through frequency offset compensation (FOC), data aided frequency domain equalization (DA FDE) and carrier phase recovery (CPR). An exact depiction of the used digital signal processing (DSP) algorithm can be found in [11]. Finally, the bit error rate (BER) is calculated to quantify transmission quality.

III. Simulation Results

For the vibration location to be detected the peak correlation change coefficients C_{Peak} need to be distinguishable between the mean coefficients C_{Mean}. We define the hypothesis H_0: *no vibration* and H_1: *vibration present at location z*. The detection problem is then:

$$\mathbb{P}_D = \mathbb{P}\left(\frac{C_{Peak}(z)}{C_{Mean}} > \gamma \mid H_1\right), \quad (1)$$

$$\mathbb{P}_{FA} = \mathbb{P}\left(\frac{C_{Peak}(z)}{C_{Mean}} > \gamma \mid H_0\right), \quad (2)$$

where γ is the detection threshold, $\mathbb{P}_D$ is the detection probability and $\mathbb{P}_{FA}$ is the probability of false alarm. In Fig. 2a) the upper introduced decision rule ratio is illustrated with an example of a phase change over 25 traces recorded at high channel signal to noise ratio (SNR) (20 dB) and high STPR (20 dB) for different transmitter laser linewidth. The location of the vibration event at 4.2 km can be clearly detected for linewidths of 100 Hz and 1 kHz. For higher linewidth the change in correlation over multiple repeated traces resembles the detected trace profile, because the laser noise decorrelates the repeated traces. This emphasizes the necessity for reduced-linewidth lasers in ISAC system development relative to those employed in conventional coherent systems.

In Fig. 2b) the detection threshold γ, as shown in (1), is depicted in dependency of the STPR and channel SNR. It is seen that the detection threshold is low for negative STPR and increases with higher STPR. The desired value of γ will depend on the cost function and the application of the ISAC system. For a low γ, where the cost factor of $\mathbb{P}_{FA}$ is small, in i.e. traffic monitoring, the STPR is set to maximize transmission quality. Whereas for a high γ, where the cost factor of $\mathbb{P}_{FA}$ is large, in i.e. intrusion detection it is vital to optimize the tradeoff of transmission quality and sensitivity by tuning the STPR. Fig. 2c) shows the SNR tolerance in the receiver of the communication link in dependence on the STPR for different transmitter laser linewidth. SNR tolerance is given as the penalty at the pre forward error control (FEC) BER threshold at 2e-2 compared to the same communication signal with no sensing probe. The result shows that the sensing probe jeopardizes the communication link significantly if the STPR is higher than 10 dB.

IV. Experimental Results

Fig. 2d) shows the experimental setup used to validate the previous simulation results. The same ISAC DSP shown in Fig. 1) is used to create the 4x8GBd PDM-QPSK signal with the sensing probe in the spectral width, which is then modulated onto the optical carrier centered at 1550 nm. The light from an external cavity laser (ECL) (linewidth < 5kHz) is split with a polarization maintaining splitter and one half is fed to the sensing receiver and the other half to the optical modulator. After 25 km of fiber a variable optical attenuator (VOA) is placed to enable the assessment of transmission quality. The communication signal is detected in the coherent receiver, which has four TIAs to amplify the current from the photodiodes. After conversion to the digital domain through a 256 GSa/s real time oscilloscope (RTO) and offline DSP processing, as depicted in the previous section, the communication signal is assessed in BER. By variation of the attenuation in the VOA the sensitivity penalty, with the pure

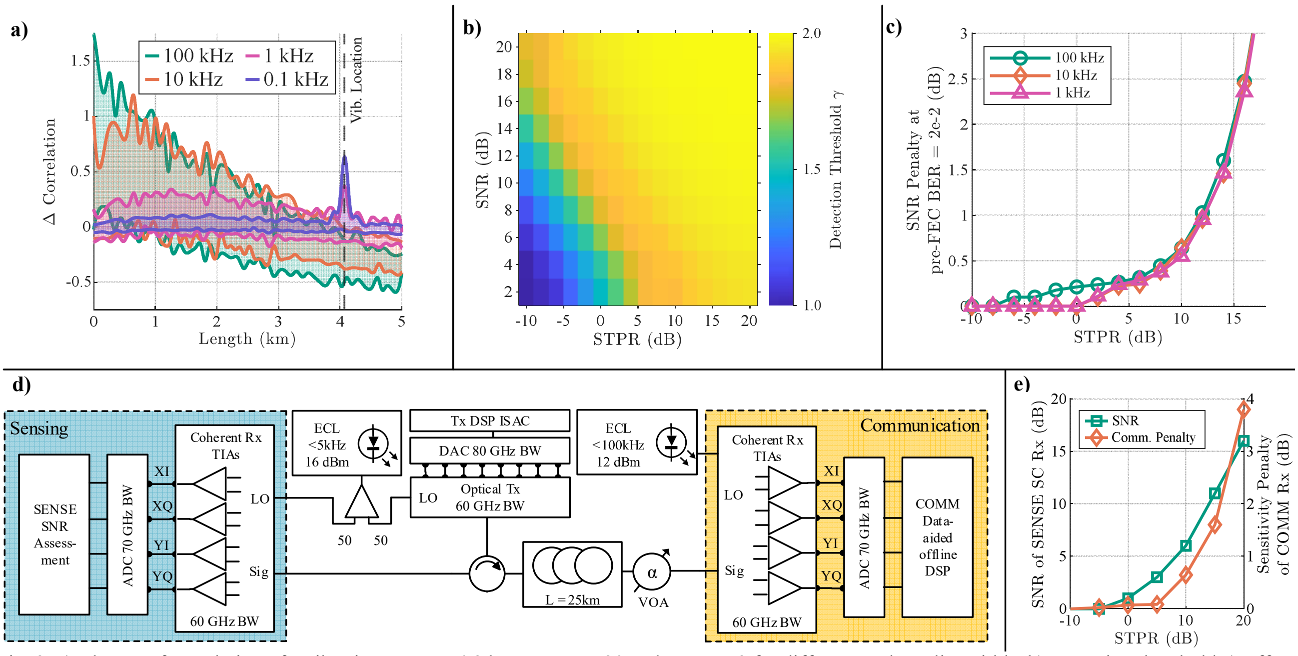

Fig. 2: a) Change of correlation of a vibration event at 4.2 km at SNR = 20 and STPR = 2 for different Tx laser linewidths b) Detection threshold c) Effect of STPR on the SNR penalty in comparison to the same signal without any sensing probe for different linewidths d) Setup for experimental verification. The coherent Rx was used alternating to receive the communication and sensing part. e) Experimentally obtained sensing SNR and induced penalty on the communication signal from the sensing subcarrier. Note: COMM = 4x8 GBd PDM-QPSK. SENSE = 500 MBd PDM-BPSK.

communication signal without inserted sensing probe as a baseline, is evaluated for different STPR. The results are shown in Fig. 2e), where the penalty in BER coincides with the results obtained by simulation. When the launch power of the sensing subcarrier exceeds the launch power of the communication carrier by more than 5 dB the sensing subcarrier impairs the detection of the communication signal. Consequently, the receiver detection sensitivity exhibits degradation of up to 3.8 dB at an STPR of 20 dB. The sensing receiver detects the backscattered signal from the link coherently and the SNR of the sensing subcarrier is calculated digitally in the DSP. Fig. 2e) illustrates the received SNR as a function of STPR. For negative STPR values, the sensing channel exhibits degraded SNR performance, but for positive STPR, the received SNR increases, reaching 16 dB at an STPR of 20 dB. Note that, because of the memory limitation in the 80 GSa/s digital to analog converter (DAC), we restrict ourselves here to report the SNR of the sensing pulse. The only amplification used to characterize the SNR is the TIA in the coherent Rx, which highlights the strong use case for integrated DAS and communication in coherent PONs.

V. Conclusion

We confirmed experimentally a method to insert DAS probes into the spectral gap between two neighboring subcarriers of downstream communication subcarriers in coherent PON. The signal can be jointly detected with the upstream traffic, which enables the integration of DAS data acquisition into OLT transceivers. The acquired probe data enables efficient monitoring of numerous feeder fibers deployed in urban access network infrastructures. We provide a tradeoff analysis for the power allocation of sensing signal and communication signal in the subcarrier multiplexing stage at the transmitter side and evaluate analytically and experimentally the impact of the sensing signal on the downstream communication signals when the total power is limited by the maximum output power of the transmitter.

Acknowledgment

This work was partly funded by the BMFTR funded project SUSTAINET-Innovate (grant no. 16KIS2261).

References

[1] T. Koonen, "Fiber to the Home/Fiber to the Premises: What, Where, and When?," in *Proceedings of the IEEE*, vol. 94, no. 5, pp. 911-934, 2006.

[2] E. Ip *et al*., "Distributed fiber sensor network using telecom cables as sensing media: technology advancements and applications [Invited]," in *Journal of Optical Communications and Networking*, vol. 14, no. 1, pp. A61-A68, 2022.

[3] J. Liu *et al.*, "Urban sensing using existing fiber-optic networks." *Nature Communications*, vol. 16, no. 1, pp. 3091, 2025.

[4] C. Dorize *et al.*, "From Coherent Systems Technology to Advanced Fiber Sensing for Smart Network Monitoring," in *Journal of Lightwave Technology*, vol. 41, no. 4, pp. 1054-1063, 15 Feb.15, 2023.

[5] J. Wang *et al.*, "High-efficiency ISAC to enable sub-meter level vibration sensing for coherent fiber networks," *2024 Optical Fiber Communications Conference and Exhibition (OFC)*, San Diego, CA, USA, 2024, pp. 1-3.

[6] I. B. Kovacs *et al.*, "Simplified coherent optical network units for very-high-speed passive optical networks," in *Journal of Optical Communications and Networking*, vol. 16, no. 7, pp. C1-C10, 2024.

[7] Y. Luo and F. Effenberger, "What is beyond 50G: future standards of optical access networks [Invited]," in *Journal of Optical Communications and Networking*, vol. 16, no. 7, pp. C106-C112, 2024.

[8] H. Zhang *et al.*, "Adaptive TFDM coherent PON: a flexible architecture with variable modulation formats and baud rates for next-generation optical access networks," in *Journal of Optical Communications and Networking*, vol. 17, no. 7, pp. C11-C21, 2025.

[9] M. Brown. "Simulation of coherent phase optical time-domain reflectometry," M. S. thesis, University of Manitoba, Winnipeg, MB, 2017.

[10] E. Säckinger, *Analysis and design of transimpedance amplifiers for optical receivers*. Hoboken, NJ, USA : Wiley, 2017.

[11] R. Elschner *et al.*, "Data-Aided DSP for Flexible Transceivers", *Advanced Photonics Congress, paper: SW1C.1 (invited)*, San Diego, 2014